

## **Controlling and Modelling of an EV Charging Station with PV and Battery using ANN Control**

**C. SUNIL TEJA<sup>1</sup>, K. JITHENDRA GOWD<sup>2</sup>, Y. MANASA<sup>3</sup>**

<sup>1</sup> PG-Scholar, Department of EEE (Electrical Power System), JNTUA College of Engineering, Ananthapuramu.,A.P., India.

<sup>2</sup> Associate Professor, Department of EEE, JNTUA College of Engineering, Ananthapuramu., A.P., India.

<sup>3</sup> Assistant Professor, Department of EEE, JNTUA College of Engineering, Ananthapuramu., A.P., India.

### **Abstract:**

Renewably powered fast-charging stations need to be affordable, efficient and consistent to meet the charging demand of most licensed electric vehicles. Super-fast charging stations, however, could strain the electrical system by producing voltage drops, unexpected power outages, and overload during peak hours. This paper presents an intricate portrayal of a converter-driven EV charging hub harmonized with PV power creation and battery energy storage unit managed by Artificial Neural Networks (ANN). Within this endeavor, the ANN control concept along with the fusion of PV power generation, EV charging hub, and Battery Energy Storage (BES) delivers enhanced stability through power discrepancy alignment, peak reduction, valley enrichment, and voltage dip compensation. Therefore, the impact on the power grid diminishes as a result of aligning the daily charging needs with the ample daytime PV output. To avert voltage fluctuations and ensure a consistent electricity supply for both PV systems and electric vehicles, a innovative BES controller is set to be created. By following the proposed control plan, the BES will discharge when there's inadequate PV power for local EV charging and charge when there's excess PV energy or low demand on the power grid, like during nighttime. Hence, a comprehensive energy solution is achieved through the integration of EV charging, PV generation, artificial neural network logic, and a BES.

Keywords: PV, ANN, BES, EV charging station

### **1. Introduction:**

Electric vehicles (EVs) are becoming increasingly popular as environmentally friendly alternatives to conventional gasoline-powered cars. This surge in EV adoption, however, highlights the need for an extensive network of charging stations, due to the relatively short battery ranges. This, in turn, poses challenges such as putting stress on the power grid and potentially causing instability. Explore the combination of photovoltaic power generation and electric vehicle charging to improve energy usage during peak hours.

Battery energy storage (BES) is expected to maintain DC bus voltage, balance power difference and smooth PV equipment due to solar energy interaction. Due to the limited capacity of EV batteries, the development and use of EVs requires the provision of broadly supplied charging stations [2]. But widespread direct charging facilities, particularly those that are quick and extremely quick, have increasing demands on the safety and consistency of the power grid, and look problems such as high demand, voltage drops, and power differences [3]. Exploring the fusion of

photovoltaic (PV) generation and EV charging infrastructure aims to enhance power utilization during peak periods. Utilizing battery energy storage (BES) for controlling DC bus voltage, managing power discrepancies, and stabilizing PV power output in response to solar energy variations. Due to the limited capacity of the batteries, the transmission of electric vehicles requires a connection between charging stations. However, because they might result in power imbalances, voltage fluctuations, and peak demand surges, the widespread installation of grid-connected charging stations—especially fast and ultrafast ones—poses a threat to system stability and reliability.

While some scholars have delved into merging PV generation with EV charging infrastructure, PV integration remains a minor contributor to power supply for charging stations in academic studies. Given the escalating need for rapid charging during daylight hours, the rapid expansion of PV generation optimizes power consumption during peak periods by capitalizing on ample daytime energy production. To address the intermittent nature of PV power generation, battery energy storage (BES) can be used to control the DC bus or load voltage, eliminate power imbalance, and stabilize the PV power output. In this study, which explores the better power density and effectiveness of multiport power converters, a multiport DC-DC converter is used for electric vehicle charging stations instead of using three separate DC-DC converters. According to the study, the charging station configuration can be divided into two main topologies: AC bus-based or DC bus-based. Since the output of PV and BES can be considered as DC sources, DC bus-based charging stations are chosen to improve

solar energy efficiency and reduce the costs and losses associated with inverters. Unlike isolated multiport converters, non-isolated multiport converters, which are usually derived from buck or boost converters, are more compact in design, have higher power density and higher efficiency than isolated converters. In summary, the focus and contributions of this study can be explained as follows: Initially, the integration of PV and BES, rather than relying solely on the grid, was recognized as the main power source for EV charging. Subsequently, the complex operation modes, control strategies and interactions between PV system, BES, power grid and EV charging are formalized and explored in the context of high-level integration of PV system and extensive EV charging infrastructure. Furthermore, a comprehensive analysis of power losses and efficiency comparisons is conducted. SiC switches with a non-isolated structure are preferred for increased efficiency and decreased losses in the EV charging station, whereas multiport power converters are preferred for their high-power density and efficiency. Because of their small batteries, EVs are becoming more and more commonplace, which means that charging stations must be installed everywhere. The study explores how PV and BES are used to power EV charging at the forefront, creating complex operational plans, control schematics, and effectiveness evaluations that contrast Si and SiC EV stations. The work investigates the methodical modelling of a battery energy storage system with ANN regulation and a multiport converter-centric EV charging station connected to PV power generation. Within this endeavour, the employment of ANN regulation, in conjunction with PV power generation, an EV charging facility, and Battery Energy

Storage (BES), bolsters stability by harmonizing power discrepancies, minimizing peak and trough loads, and rectifying voltage fluctuations. Therefore, the power grid experiences a reduced impact because of aligning daily charging needs with ample daytime PV output. A control unit for the Battery Energy Storage (BES) will be devised to eradicate voltage fluctuations and ensure a steady power supply for both PV and EV systems. In times of surplus PV energy or low grid demand, such as during the night, the BES will commence charging, following the recommended control mechanism. Conversely, the BES will discharge when PV generation falls short for local EV charging requirements. Ultimately, a holistic energy solution is provided through the integration of EV charging, PV generation, Artificial Neural Network (ANN) logic, and a BES system. II. Methodology:

The proposed approach embodies a methodology comprising several key elements. At its core lie PV, BES, and EV, forming the main components of the system. The paper at hand pertains to software development, with MATLAB Simulink software being the primary tool utilized. This innovative technique is harnessed for a specific methodological purpose.

**Case 1- PV TO EV:** The primary purpose of solar cells is to generate electricity using solar energy. The electric car is directly charged with the daytime electricity generated.

**Case 2 – BES TO EV:** Photovoltaic cells produce electricity and store it in the form of cells (battery energy). When we need electricity to charge electric cars, the

battery sends electricity directly to the electric car.

### Topology of plug-in electric vehicle chargers:

Three distinct converters are used to link the three power sources—photovoltaic (PV), electric car charger, and AC grid—in conventional DC bus charging stations with PV integration (See Fig. 1). Incorporating a second bidirectional power source, Battery Energy Storage (BES) becomes part of the innovative DC bus charging station. The BES plays a crucial role in stabilizing the DC link voltage and addressing any power surplus or deficit from the PV system. Delve into a detailed exploration of the setup's operation and various modes in the ensuing discussion.

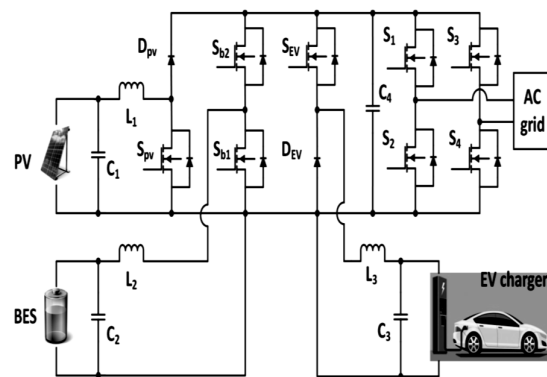


Fig 1: PEV charger topology

#### b. Photovoltaic Array Modelling:

The cellular unit plays a vital role in the intricate web of PV electrical activities. Solar PV systems utilize solar cells, and their interconnected areas arranged in a series or parallel configuration to enhance current, power, and voltage. In practical scenarios, each cell operates akin to a diode, with the junction marked by the semiconductor material. At this juncture, the lightweight load is embraced by the captivating electrical force, swiftly

dispersing the currents. Illustration 2 showcases the (current-voltage) and (Power-Voltage) traits under various celestial light strengths of the PV exhibit, while fig 5 highlights the widespread availability of numerous power points on every output.

$$I = I_{ph} - I_D - I_{sh} \text{---(1)}$$

$$I = I_{ph} - I_0 \left[ \exp\left(\frac{qV_D}{nKT}\right) - \left(\frac{V_D}{R_s}\right) \right] \text{---(2)}$$

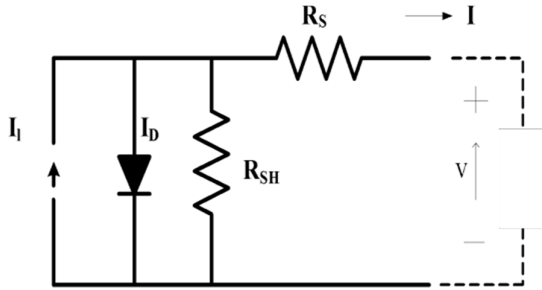


**Fig 2: PV Electrical Equivalent circuit**

### Operation of Multistage Converter:

#### Case 1: PV to EV:

In this configuration, if SEV is enabled, switches Spv, Sb<sub>1</sub>, and Sb<sub>2</sub> are disabled. As a result, PV provides electricity to the load directly. Differential equations for this stage can be expressed as follows:

$$i_{pv} = C_1 \frac{dV_{c1}}{dt} + i_{EV} \text{---(4)}$$

$$C_2 \frac{dV_{c2}}{dt} = \frac{v_{BAT} - v_{c2}}{rb} - i_{L2} \text{---(5)}$$

$$i_{EV} = C_3 \frac{dV_{c3}}{dt} + \frac{v_{EV}}{R_{EV}} \text{---(6)}$$

$$V_{c1} - V_{c3} = L_3 \frac{dI_3}{dt} \text{--- (7)}$$

$$L_2 \frac{dI_2}{dt} = -v_{c2} \text{--- (8)}$$

where C<sub>1</sub>, C<sub>2</sub>, C<sub>3</sub>, L<sub>1</sub>, L<sub>2</sub>, L<sub>3</sub>, and rb express as the corresponding obstruction between VBat and C<sub>2</sub>, the inductance of the

PV port inductor, the inductance of the BES port inductor, the inductance of the EV load port inductor, and the capacitance of the EV port capacitor for each of the four scenarios. respectively, as appeared in Fig. 1; i<sub>PV</sub>, i<sub>EV</sub>, i<sub>L2</sub>, and i<sub>L3</sub> speak to the output current from PV boards, the current of EV load, the current through inductor L<sub>2</sub>, and the current through inductor L<sub>3</sub>, individually.

The duty cycle of the operating switch Spv is given as

$$\frac{V_{DC}}{V_{PV}} = \frac{1}{1 - D_{pv}} \text{---(3)}$$

#### 2. Case 2: BES to EV

Table 1 shows that when Sb<sub>1</sub> and Sb<sub>2</sub> are disabled and Spv and S<sub>EV</sub> are ON, BES discharges to the EV load. Differential equations in this context can be expressed as:

$$i_{pv} = C_1 \frac{dV_{c1}}{dt} \text{---(9)}$$

$$L_2 \frac{dI_2}{dt} = v_{dc} - v_{c2} \text{---(10)}$$

$$v_{dc} - v_{c3} = L_3 \frac{dI_3}{dt} \text{---(11)}$$

$$C_2 \frac{dV_{c2}}{dt} = \frac{v_{BAT} - v_{c2}}{rb} - i_{L2} \text{--- (12)}$$

$$i_{EV} = C_3 \frac{dV_{c3}}{dt} + \frac{v_{EV}}{R_{EV}} \text{---(13)}$$

#### Case 3: PV to BES:

The PV surplus energy is used to charge the BES when Sb<sub>2</sub> is turned on and Sb<sub>1</sub>, Spv, and S<sub>EV</sub> are OFF. The differential equations in this mode can be expressed as follows:

$$i_{pv} = C_1 \frac{dV_{c1}}{dt} - i_{L2} \text{---(14)}$$

$$L_2 \frac{dI_2}{dt} = v_{dc} - v_{c3} \text{---(15)}$$

$$v_{dc} - v_{c3} = L_3 \frac{dI_3}{dt} \text{---(16)}$$

$$C_2 \frac{dV_{c2}}{dt} = \frac{v_{BAT} - v_{c2}}{rb} - i_{L2} \text{--- (17)}$$

$$i_{EV} = C_3 \frac{dV_{C3}}{dt} + \frac{v_{EV}}{R_{EV}} \text{---(18)}$$

The duty cycle for the switch Sb2 can be obtained with:

$$\frac{v_{BAT}}{v_{dc}} = D_{b2} \text{---(19)}$$

where Db2 represents the duty cycle of the switch Sb2.

**PV to BES, Grid to EV, and PV to Grid:**

By using above differential equations can be summarized by using cases 1 to 3

| $S_{pv}$ | $S_{b1}$ | $S_{b2}$ | $S_{EV}$ | Power flow |
|----------|----------|----------|----------|------------|
| off      | off      | off      | on       | PV to EV   |
| off      | off      | on       | off      | PV to BES  |
| on       | off      | off      | on       | BES to EV  |
| —        | on/off   | off/on   | on       | Grid to EV |
| off      | off      | off      | off      | PV to grid |

Table 1 : Ev charging operating switches

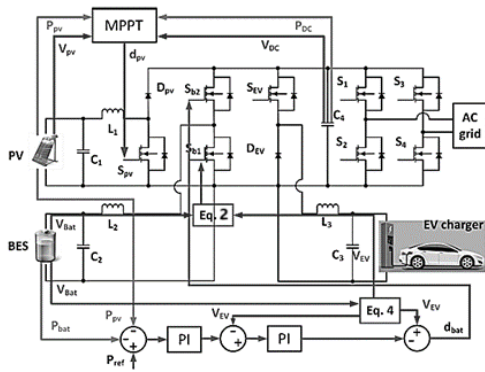


**Fig 3:** Block Diagram of PV based V2G System

**III. Simulation Results:**

The MATLAB software's Simulink tool is utilized for conducting simulation studies on the proposed system. The photovoltaic (PV) array is modelled using its standard mathematical equation. The multiport converter is represented using power MOSFETs, inductors, capacitors, the solar array, and various icons available in the Sim

Power Systems Block set within the Simulink library. The Simulink library contains many components that are utilized in the development of the controller, including a comparator, multiplier, PWM generator, pulse generator, logic gates, and PI controller as shown in Fig 3.

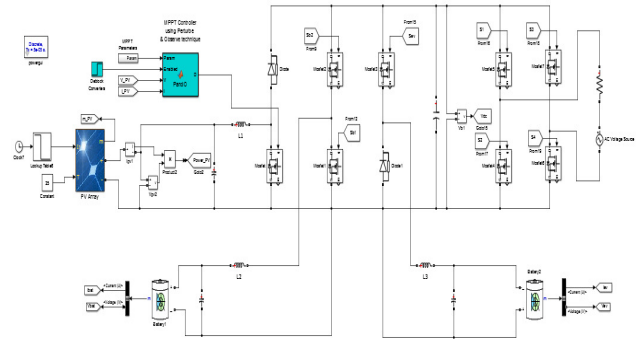


**Fig 4:** Simulation Diagram for PV based V2G System

Maintaining the load voltage and controlling the power gap are the two main functions of the BES regulator (Fig. 5).

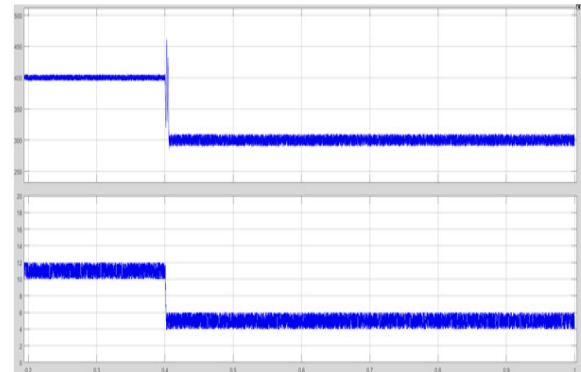


**Fig 5 :** The simulation results of (a) PV Voltage (b) PV Power.

Photovoltaic panels can charge electric cars when the sun shines. When photovoltaic electricity is too much, photovoltaic energy is charged locally and used locally. When photovoltaic power is not enough, such as partial shading or other bad conditions, photovoltaic power will start and collect the energy difference

between photovoltaic power and electric car. Fig 5 displays the simulation results for the voltage, demand, and power consumption of an EV charging terminal. During the simulation from 400 ms to 700 ms, the photovoltaic panels can produce 5.7 kW of energy, which is enough to meet the capacity of the electric vehicles. Therefore, the framework works in PV for EV mode and the BES does not need to be charged/discharged. When the demand increases to 700 ms, the photovoltaic panels cannot provide the full 7.7 kW charging power required in 500 irradiances. Since then, the BES started to advertise electric vehicles that provide 2 kW of power and provide electrical support.

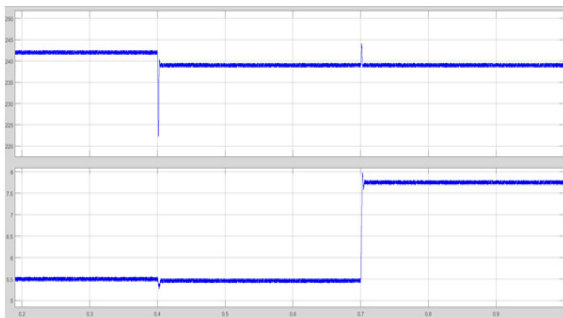


**Fig 6.:** The simulation results of EV charging, (a) the terminal voltage of the EV charger (b) the demand and consumed power of EV charging.

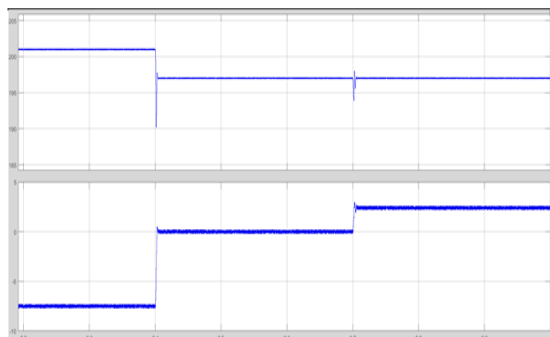


**Fig 7.** The simulation results of the BES, (a) the terminal voltage of the BES, (b) the output power from BES.

### 3.1 Using ANN:

Artificial neural networks (ANNs) can be simply converted into a set of if-then rules, while ANN systems can be thought of as a neural network structure with knowledge dispersed across connection strengths when they are combined. Research and application of neural and ANN inference methods have shown the advantages of combining neural and ANN systems, especially in areas such as direct extension of ANN algorithms and direct transfer of knowledge expressed according to the rules of the ANN language. Using hybrid learning, adaptive systems establish the parameters of Sugeno-type ANN inference systems. It uses a combination of least-squares and back-propagation gradient descent to learn the FIS membership function parameters to replicate a given training data set. There are two main learning phases in the network. The critical parameters define the least squares estimate as the learning process progresses. Error signals travel from the output layer to the input layer during the backward phase. These signals are derivatives of the squared error about each node's output. In this step back in time, the gradient descent algorithm modifies the premise parameters. For the neural network to successfully match the training data, it must determine the right parameter values during the learning or training phase. It is possible to lower the error rate of ANN training by employing several tactics. To find the ideal parameters more efficiently, we combine the gradient descent methodology with a least squares method.

#### 3.1.1 Architecture of ANN

In an adaptive network configuration, each node function is a parameterized function with tunable parameters that change the node functions and the overall behavior of

the adaptive network. A static node function is applied to the incoming signals to create a single node output. The five layers that make up the overall system architecture are represented in "FIG 8" and are the "ANN layer," "product layer," "normalized layer," "de-ANN" layer, and "total output" layer.

An ANN inference system (FIS) with an input/output system (FIS) and a set of parameters is illustrated by the ANN approach. The parameters of the membership function are tuned (adjusted) using either a backpropagation algorithm by itself or in combination with a least squares-style method. The ANN looks for the sweet spots for the parameters of a comparable ANN inference system using a learning technique. To reduce the divergence from the ideal output, the parameters are tuned during the training phase. We use a hybrid technique for optimization that benefits from both gradient-descent and least-squares methods.

The premise parameters in ANN are the ones you should adjust till they're ideal. The membership functions' format is specified by these parameters. After MFs are generated, several optimization strategies can be used to lower the error measure. ANN systems can learn from the data they are modelling thanks to the parameter set of an adaptive network. We assume for the purposes of this study that the adaptive system under investigation has two inputs,  $V_1$  and  $V_2$ , and one output,  $f$ .

Examining a Takagi, Sugeno, and Kang (TSK) ANN inference system of the first order with two rules:

Rule 1: if ( $v$  is  $V_1$ ) and ( $d$  is  $D_1$ ) then  $f_1 = p_1v + q_1d + r_1$

Rule 2: If ( $v$  is  $V_2$ ) and ( $d$  is  $D_2$ ) then  $f_2 = p_2v + q_2d + r_2$

Where  $p_1, p_2, q_1, q_2, r_1$  and  $r_2$  are linear parameters and  $V_1, V_2, D_1$  and  $D_2$  are non-linear parameters, in which  $V_1$  and  $D_1$  are the membership functions of ANN (antecedent). We employ both the circle and the square to portray flexible talents. Nodes depicted as circles cannot have their parameters altered during adaptation or training, but nodes depicted as squares can. ANN logic and neural networks are used to form ANN. It is crucial to fine-tune the amount of training epochs, membership functions, and ANN rules used in the development of an ANN model. Precise mapping of such parameters is extremely important because there is a chance that the system will either fit the data too much or not at all. To accomplish this modification, a single algorithm that combines the mean-square-error method, gradient descent, and the least-squares approach can be used. The system performs better when the difference between the target and ANN results is smaller. Consequently, we concentrate on reducing errors produced during the training process. The outcome of this planned and developed integration are ANN neural networks (FNNs); generally speaking, the combination of ANN logic and the neural network is referred recognized as an ANN.

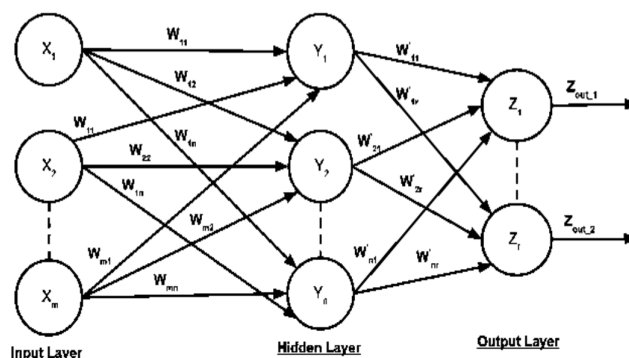


**Fig 8:** Basic architecture of ANN

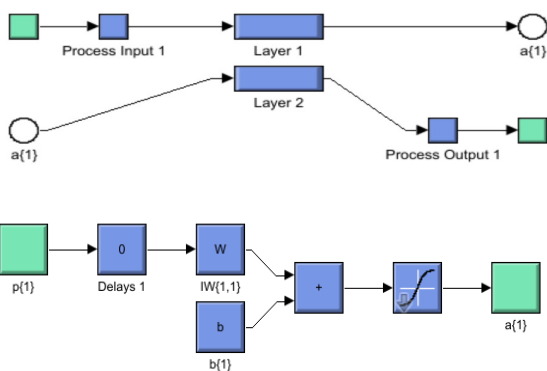


**Fig 9:** Training process for ANN controller.

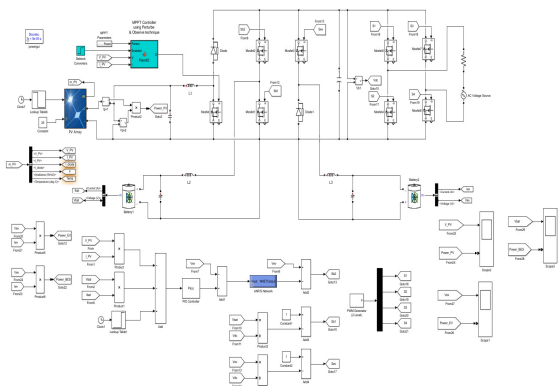


**Fig 10:** Proposed system simulation

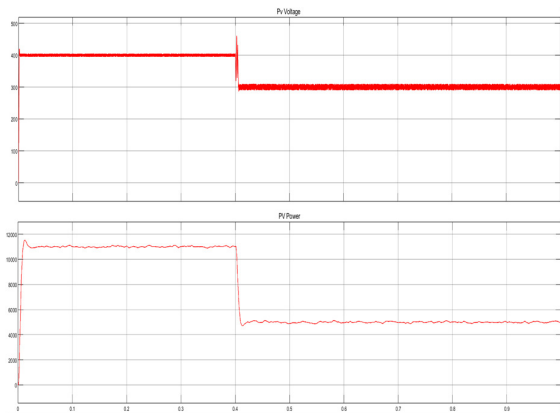


**Fig 11 :** (a) the output voltage of the PV panels (b) the output power from the PV panels.

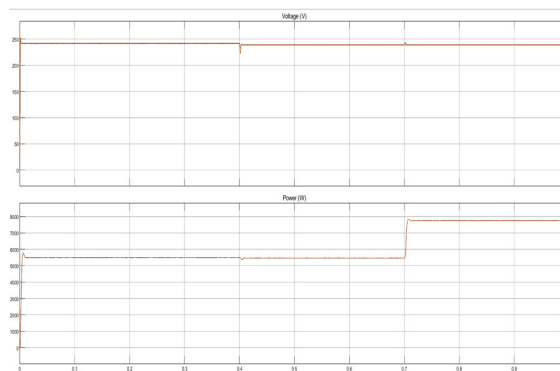


**Fig 12 :** The simulation results of EV charging, (a) consumed power of EV charging, (b) the terminal voltage of the EV charger.

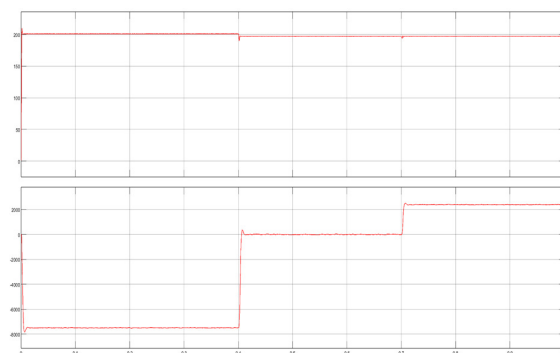


**Fig 13:** The simulation results of the BES, (a) the BES's output power (b) the BES's terminal voltage.

The suggested control architecture uses a battery energy storage (BES) controller when local EV charging cannot be accomplished with photovoltaic (PV) output alone. Then, during periods of low power grid demand, such as at night, or when PV output is excess, the BES controller begins charging. Combining PV generation, BES, and EV charging improves grid dependability and stability.

After studying the various working modes and their advantages, MATLAB/Simulation thermal and simulation models of multiport converter-based EV charging stations and the suggested Sic counterpart were created. The results of the simulation suggest that



the three cases (PV-to-EV, PV-to-BES, and BES-to-EV) efficiency could be greater under typical operating conditions when compared to Si-based EV charging stations.

### Conclusion:

This proposal proposes a multiport converter EV charging station with PV and BES, utilizing ANN control. The purpose of a BES controller is to control voltage sag to balance the power difference between PV generation and the needs for EV charging. When there is nighttime valley demand in the power grid or when there is excess PV generation, BES begins charging. This is how the recommended control strategy operates. When local EV charging demands more power than PV can supply, BES releases energy. As a result, EV charging, PV output, BES, and ANN all cooperated.

### REFERENCES

- [1] V. Rallabandi, D. Lawhorn, J. He, and D. M. Ionel, "Current weakening control of coreless farm motor drives for solar race cars with a three-port bi-directional dc/dc converter," in *2017 IEEE 6th International Conference on Renewable Energy Research and Applications (ICRERA)*, Nov 2017, pp. 739–744.
- [2] Y. Liu, Y. Tang, J. Shi, X. Shi, J. Deng, and K. Gong, "Application of small-sized smes in an ev charging station with dc bus and pv system," *IEEE Trans. on Applied Superconductivity*, vol. 25, no. 3, pp. 1–6, June 2015.
- [3] M. Ahmadi, N. Mithulananthan, and R. Sharma, "A review on topologies for fast charging stations for electric vehicles," in *2016 IEEE International Conference on Power System Technology (POWERCON)*, Sep. 2016, pp. 1–6.
- [4] J. C. Mukherjee and A. Gupta, "A review of charge scheduling of electric vehicles in smart grid," *IEEE Systems Journal*, vol. 9, no. 4, pp. 1541–1553, Dec 2015.
- [5] H. Zhu, D. Zhang, B. Zhang, and Z. Zhou, "A nonisolated three-port dc-dc converter and three-domain control method for pv-battery power systems," *IEEE Trans. on Industrial Electronics*, vol. 62, no. 8, pp. 4937–4947, Aug 2015.
- [6] A. Hassoune, M. Khafallah, A. Mesbahi, and T. Bouragba, "Smart topology of ev's in a pv-grid system-based charging station," in *2017 International Conference on Electrical and Information Technologies (ICEIT)*, Nov 2017, pp. 1–6.
- [7] B. Honarjoo, S. M. Madani, M. Niroomand, and E. Adib, "Non-isolated high step-up three-port converter with single magnetic element for photovoltaic systems," *IET Power Electronics*, vol. 11, no. 13, pp. 2151–2160, 2018.
- [8] S. Bai, D. Yu, and S. Lukic, "Optimum design of an ev/phev charging station with dc bus and storage system," in *2010 IEEE Energy Conversion Congress and Exposition*, Sep. 2010, pp. 1178–1184.
- [9] H. Zhu, D. Zhang, B. Zhang, and Z. Zhou, "A nonisolated three-port dc-dc converter and three-domain control method for pv-battery power systems," *IEEE Trans. on Industrial Electronics*, vol. 62, no. 8, pp. 4937–4947, Aug 2015.
- [10] H. Zhu, D. Zhang, Q. Liu, and Z. Zhou, "Three-port dc/dc converter with all ports current ripple cancellation using integrated magnetic technique," *IEEE Trans. on*

Power Electronics, vol. 31, no. 3, pp. 2174–2186, March 2016.

[11] SunTech Power STP235-20-Wd, <https://www.freecleansolar.com/235W-solar-panels-Suntech-STP235S-20-Wd-mono-p/stp235s-20-wd.htm>, Accessed on 2018-12-19.

[12] CREE C3M0065090 D MOSFET, <https://www.wolfspeed.com/c3m0065090d>, Accessed on 2018-12-19.